Layered niobate KNb_3O_8 synthesized by the polymeric precursor method

(Niobato lamelar KNb_3O_8 sintetizado pelo método dos precursores poliméricos)

J. K. D. de Souza[1], L. M. C. Honório[1], J. M. Ferreira[2], S. M. Torres[3], I. M. G. Santos[1], A. S. Maia[1*]
[1]Núcleo de Pesquisa e Extensão, Laboratório de Combustíveis e Materiais; [3]Departamento de Materiais, Centro de Tecnologia, UFPB, João Pessoa, PB
[2]Instituto Federal de Educação, Ciência e Tecnologia da Paraíba, João Pessoa, PB
**ary.maia@quimica.ufpb.br*

Abstract

The polymeric precursor method was used for the synthesis of KNb_3O_8 and compared to the solid-state method. The materials were characterized by X-ray diffraction (XRD), infrared spectroscopy, Raman spectroscopy, scanning electron microscopy, and determination of surface area and total pore volume by nitrogen isotherms at 77 K. The material prepared by the polymeric precursor method was single-phase while $K_2Nb_4O_{11}$ was obtained as secondary phase when the solid-state method was used, as evidenced by the XRD patterns and the Raman spectra. The morphology of the materials was significantly altered by the synthesis method, as the KNb_3O_8 prepared by the polymeric precursor method presented a more porous morphology leading to a higher surface area and pore volume.
Keywords: KNb_3O_8, polymeric precursor method, Raman spectroscopy, $K_2Nb_4O_{11}$.

Resumo

O método dos precursores poliméricos foi usado na síntese do KNb_3O_8 e comparado com o método do estado sólido. Os materiais foram caracterizados por difração de raios X (DRX), espectroscopia na região do infravermelho, espectroscopia Raman, microscopia eletrônica de varredura e determinação de área superficial e volume total de poros através de isotermas de nitrogênio a 77 K. O material preparado a partir do método dos precursores poliméricos foi monofásico enquanto o sintetizado pelo método de reação no estado sólido apresentou $K_2Nb_4O_{11}$ como fase secundária, evidenciada pelas análises de DRX e Raman. A morfologia dos materiais foi significativamente alterada pelo método de síntese, com o KNb_3O_8 preparado pelo método dos precursores poliméricos apresentando morfologia mais porosa, levando a área superficial e volume de poros maiores.
***Palavras-chave**: KNb_3O_8, método dos precursores poliméricos, espectroscopia Raman, $K_2Nb_4O_{11}$.*

INTRODUCTION

Niobates have been widely reported in the literature due to their interesting electro-optic, dielectric, piezoelectric and photocatalytic properties, which allow their use as sensors, electronic devices and photocatalysts for water splitting and for photobleaching of organic dyes [1-8]. KNb_3O_8 is a layered niobate with orthorhombic structure (space group *Aman*), whose unit cell is formed by stacking of two lamellae along the crystallographic axis c, giving rise to only one type of interlayer region. Their lamellae are formed by distorted octahedra (NbO_6) sharing vertices and edges (Fig. 1), with the lattice constants a=8.903 Å, b=21.16 Å and c=3.799 Å [5, 8].

Several papers report the synthesis of the layered KNb_3O_8 by the solid-state method [4, 10] and also by the molten salt method [5, 11]. For instance, Zhang *et al*. [4] and Bizeto *et al*. [10] used Nb_2O_5 and K_2CO_3 as precursors during synthesis by the solid-state method, with a heat treatment at 900 °C. Conventional or microwave assisted hydrothermal method were also used to synthesize KNb_3O_8 and nanometric particles were obtained [7, 12-14]. A careful evaluation of the XRD patterns indicates the formation of secondary phases for all these methods, even in small amounts, confirming the difficulty to obtain a single-phase KNb_3O_8. Chemical methods, such as the sol-gel route or the polymeric precursor method, usually lead to a greater homogenization of the cations in solution, providing a better elemental distribution in the final lattice, preventing the formation of undesired phases [15]. This work aimed to evaluate the synthesis conditions of KNb_3O_8 by the polymeric precursor method and by the solid-state method, in order to compare its structural and morphological properties.

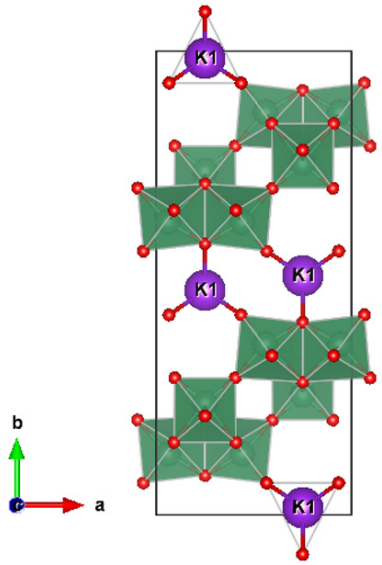

Figure 1: Schematic representation of the KNb_3O_8 unit cell, drawn by the VESTA software [9], using the atomic coordinates calculated in [8].
[Figura 1: Representação esquemática da célula unitária do KNb_3O_8, desenhada pelo programa VESTA [9], usando as coordenadas atômicas calculadas em [8].]

EXPERIMENTAL

KNb_3O_8 was synthesized by the polymeric precursor method (PP) using potassium nitrate (99%, Sigma-Aldrich), hydrated niobium ammonium oxalate (99.99%, CBMM), ammonium hydroxide (28-30%, Vetec), citric acid (99.5%, Cargill), ethylene glycol (99.5%, Vetec) and distilled water as solvent. During the PP method, the metallic citrate solutions were prepared separately using a metal/citric acid (CA) molar ratio of 1:3. The solutions were mixed, with 10% of excess of potassium, in relation to the K:Nb molar ratio in the final compound. The pH of the mixture was adjusted to 4 with NH_4OH solution followed by the temperature increase up to 70 °C. Ethylene glycol (EG) was added into the solution in the mass proportion of 60 CA:40 EG and the temperature was raised to 90 °C and maintained constant until a reduction of 2/3 of the initial volume took place. The resin was heated up to 300 °C for 2 h and then deagglomerated and sieved (200 mesh). The material was heat treated between 600 and 800 °C for 4 h, with a heating rate of 5 °C.min^{-1}. Niobium pentoxide (99.9 %, CBMM) and potassium carbonate (99%, Vetec) were used as precursors for the KNb_3O_8 synthesis by the solid-state method (SS). The powder materials were mixed in a mortar and then heated up to 1000 °C, for 9 h with a heating rate of 10 °C.min^{-1}. After periods of 1, 3, 5 and 7 h, heating was interrupted and the material was deagglomerated in a mortar, to improve the homogenization.

All materials were characterized by X-ray diffraction (XRD), Fourier-transform infrared spectroscopy (FTIR), Raman spectroscopy, scanning electron microscopy (SEM), and measurements of specific surface area and pore volume by N_2 adsorption. XRD patterns were obtained using a Shimadzu XRD 6000 instrument, using CuKα radiation (λ= 1.5418 Å) and a 2θ range of 3 to 60°. FTIR spectra were obtained with a Shimadzu IR Prestige-21 spectrophotometer, using KBr pellets. Raman spectra were obtained with a Bruker IFS 28 spectrometer with a FRA 106 FT-Raman module. SEM images were obtained in a Jeol JSM7100F microscope (10 kV) or in a FEI Quanta 450 microscope (20 kV). Specific surface area and total pore volume were determined from nitrogen adsorption isotherms at 77 K using a MicrotracBEL Belsorp-Mini.

RESULTS AND DISCUSSION

XRD patterns of the KNb_3O_8 synthesized by the PP (polymeric precursor) method (Fig. 2) showed excellent agreement with ICDD file 00-075-2182, indicating that an orthorhombic structure (space group *Amam*) was obtained. No secondary phase was observed for heat treatment temperatures up to 750 ° C, while peaks assigned to $K_2Nb_4O_{11}$, indexed in agreement with [15], were observed

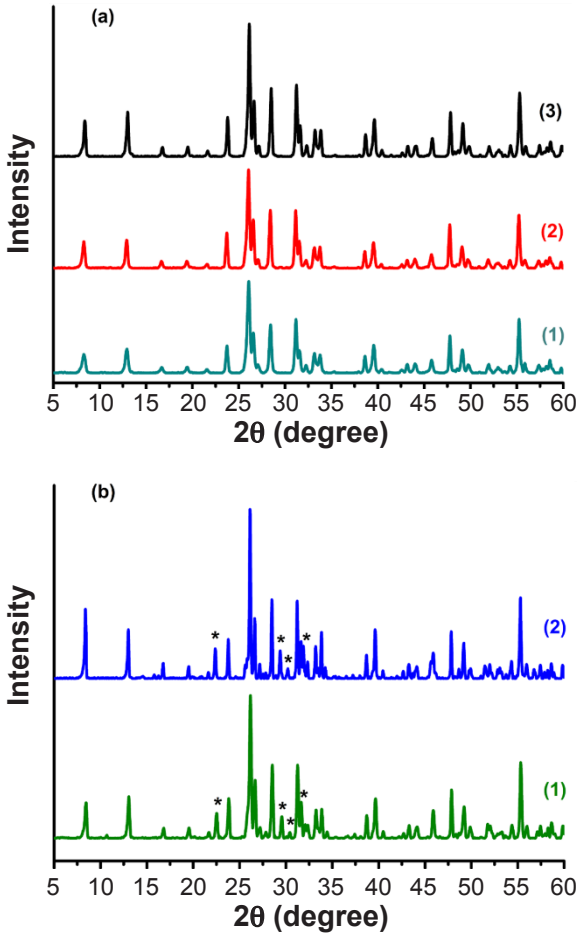

Figure 2: X-ray diffraction patterns of KNb_3O_8 synthesized by PP (polymeric precursor) method heat treated at 600 °C (a-1), 700 °C (a-2), 750 °C (a-3), and 800 °C (b-1), compared with the same material synthesized by SS (solid-state) method (b-2). * - secondary phase ($K_2Nb_4O_{11}$).
*[Figura 2: Difratogramas de raios X do KNb_3O_8 sintetizado pelo método PP (precursores poliméricos), tratado termicamente a 600 °C (a-1), 700 °C (a-2), 750 °C (a-3) e 800 °C (b-1), comparado com o mesmo material sintetizado pelo método SS (estado sólido, b-2). * - fase secundária ($K_2Nb_4O_{11}$).]*

after heat treatment at 800 °C. The same secondary phase was found in the material synthesized by the solid-state (SS) method (Fig. 2b). The secondary phase ($K_2Nb_4O_{11}$) has the tetragonal tungsten bronze (TTB) type structure, with space group *P*4/*mbm* (127). According to [15], its formation may be associated with the amount of energy required by a structural evolution mechanism, where octahedra that share edges (as observed for KNb_3O_8) assume a more stable state of energy, sharing corners (as $K_2Nb_4O_{11}$). The results found in the present article are in agreement with those reported in [15], since $K_2Nb_4O_{11}$ was observed when the heat treatment temperature of 800 °C was used in the PP method, as well as in the SS method, which used a temperature of 1000 °C.

The values of full width at half maximum (FWHM) of the (240) peak of the XRD patterns of KNb_3O_8 were calculated to evaluate the best heat treatment temperature for the PP method. Crystallinity was inferred by the relative intensity of the same peak. As shown in Table I, the increase in the heat treatment temperature from 600 to 750 °C led to the increment in crystallinity, with an evident gain in the long-range order, as indicated by the decrease of the FWHM value. Due to the absence of secondary phases and also to the greater long-range order, the sample heat treated at 750 °C was chosen for comparison with the material synthesized by the SS method using other characterization methods.

FTIR spectra presented in Fig. 3 do not show significant differences between KNb_3O_8 synthesized by the PP and the SS methods. Bands observed between 1000 and 800 cm^{-1} are in excellent agreement with literature [12, 14, 16] and were assigned to the octahedral vibrations of NbO_6. The broad absorption band around 700-400 cm^{-1} is related to the vibrations of corner-shared NbO_6 octahedra (700-600 cm^{-1}) and the structural vibrations of Nb-O (600-400 cm^{-1}) [12]. Apparently, the presence of secondary phase in the KNb_3O_8 synthesized by the SS method did not affect the set of bands observed in the FTIR spectrum.

According to literature [2, 16-19], Raman spectrum of KNb_3O_8 is characterized by two well-defined regions of Nb-O stretching modes. The first one is composed by bands at around 850-1000 cm^{-1}, which are associated with the Nb-O short bond present in highly distorted NbO_6 octahedra. The second one is located between 500 and 800 cm^{-1}, and is related to the slightly distorted NbO_6 octahedra [16-19]. Comparison between the Raman spectra of materials synthesized by PP and SS methods (Fig. 4) indicates similar profiles, except for the bands at 689, 718, 816 and 934 cm^{-1}, observed only for the material synthesized by the SS method. These four vibration bands are probably related with the secondary phase $K_2Nb_4O_{11}$, detected in the XRD patterns. Unfortunately, no literature data describing the Raman spectrum of $K_2Nb_4O_{11}$ was found in literature, but it can be observed that these bands are observed at a region associated with slightly distorted octahedra, characteristic of this phase [12, 16-18].

SEM images of the KNb_3O_8 synthesized by the two different methods (Fig. 5) show the same lamellar morphology, but with some distinct characteristics. While the material synthesized by the SS method presented a denser morphology with a smooth surface similarly to the results

Table I - FWHM value and relative intensity (I_R) of the KNb_3O_8 synthesized by the PP method heat treated at different temperatures.
[Tabela I - Valor de FWHM e intensidade relativa (I_R) do KNb_3O_8 sintetizado pelo método PP, tratado termicamente em diferentes temperaturas.]

Temperature	FWHM (°)	I_R (%)
600 °C	0.31	64
700 °C	0.26	67
750 °C	0.23	100

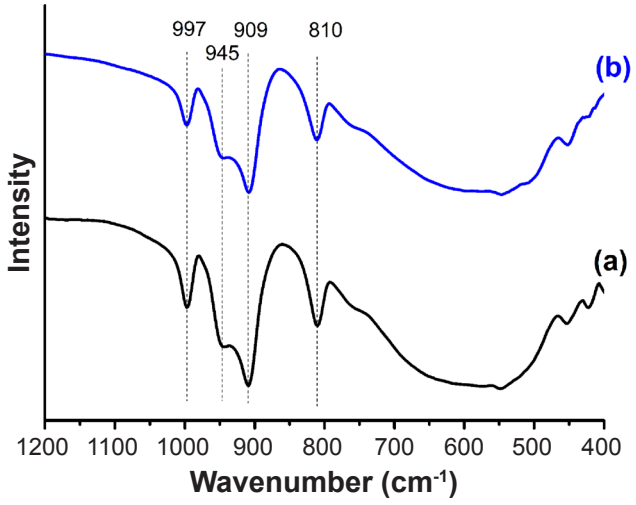

Figure 3: FTIR spectra of KNb_3O_8 synthesized by: (a) PP method heat treated at 750 °C; and (b) SS method.
[Figura 3: Espectros de FTIR do KNb_3O_8 sintetizado por: (a) método PP tratado termicamente a 750 °C; e (b) método SS.]

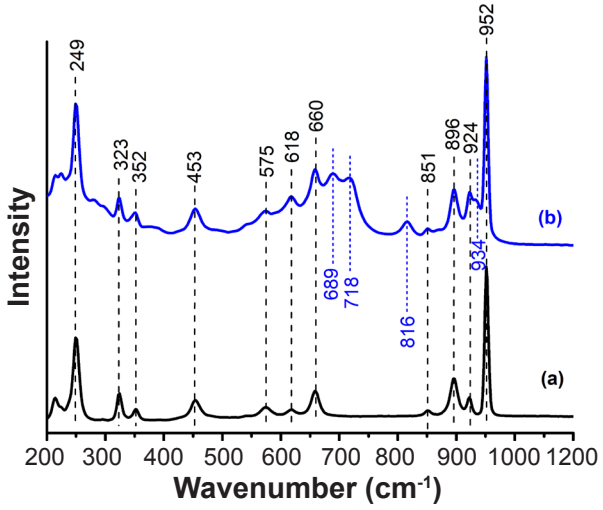

Figure 4: Raman spectra of KNb_3O_8 synthesized by: (a) PP method heat treated at 750 °C; and (b) SS method. Values presented above spectrum b are related to KNb_3O_8, while below are related to $K_2Nb_4O_{11}$.
[Figura 4: Espectros Raman do KNb_3O_8 sintetizado por: (a) método PP tratado termicamente a 750 °C; e (b) método SS. Valores acima do espectro b são relativos ao KNb_3O_8, enquanto os abaixo são relacionados ao $K_2Nb_4O_{11}$.]

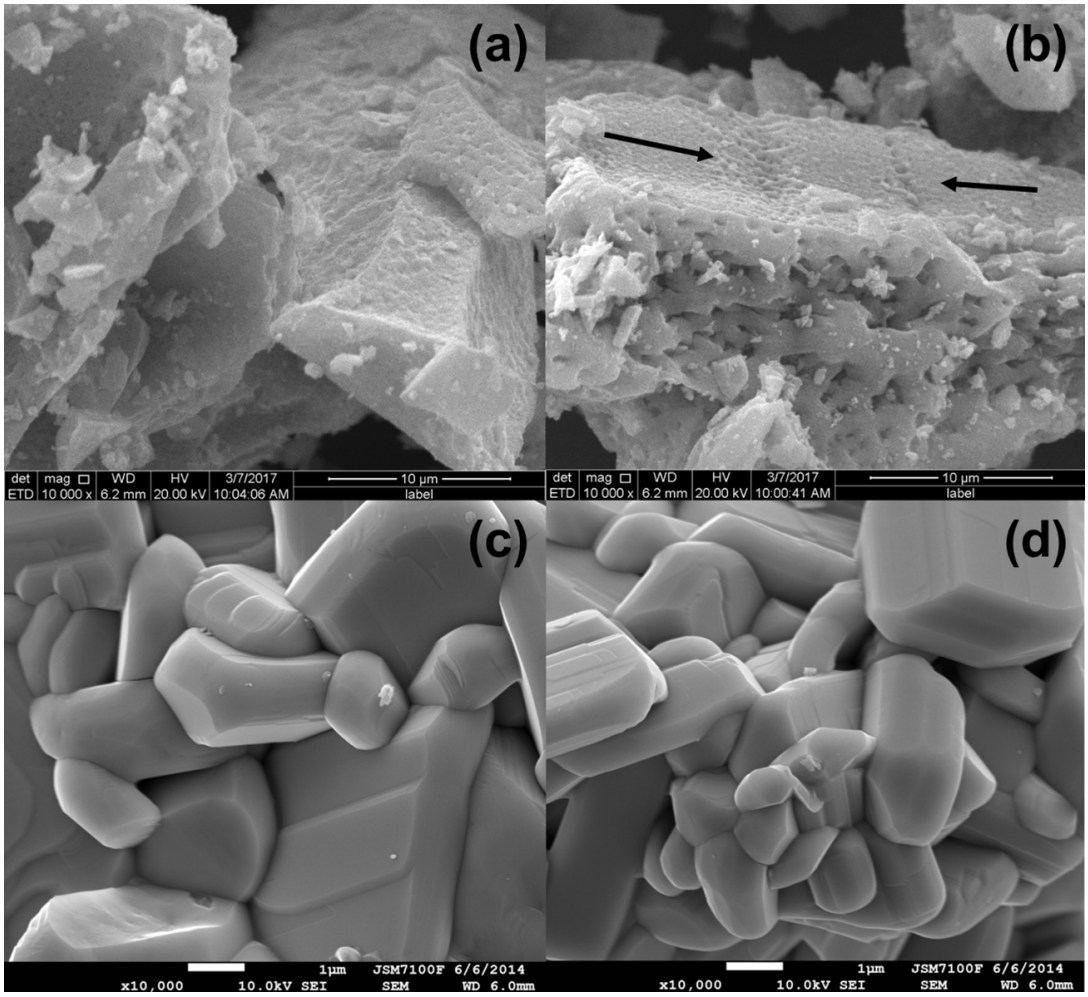

Figure 5: SEM micrographs of KNb_3O_8 synthesized by: (a,b) PP method heat treated at 750 °C; and (c,d) SS method.
[Figura 5: Micrografias obtidas por microscopia eletrônica de varredura do KNb_3O_8 sintetizado por: (a,b) método PP tratado termicamente a 750 °C; e (c,d) método SS.]

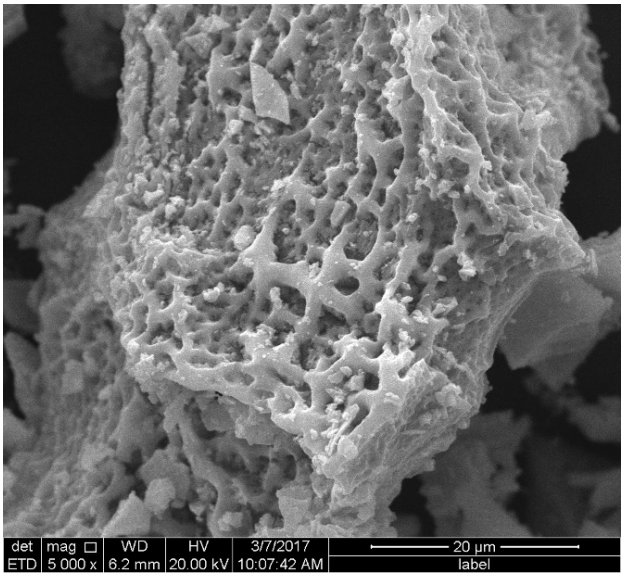

Figure 6: SEM image of KNb_3O_8 synthesized by PP method heat treated at 750 °C.
[Figura 6: Imagem de MEV do KNb_3O_8 sintetizado pelo método PP, tratado termicamente a 750 °C.]

presented in the literature [15] (Figs. 5c and 5d), the material synthesized by the PP method showed an irregular surface and large pores with diameters between 0.5 and 1 µm in the plane perpendicular to the lamella growth axis (Figs. 5a and 5b). Evidence of coalescence between grains is also observed as highlighted by arrows in Fig. 5b. During the synthesis of materials by the PP method a large amount of organic matter was used, which was eliminated by a combustion reaction during heat treatments, with the formation of a porous structure, as evidenced in Fig. 6.

BET surface area (S_{BET}) and total pore volume (V_p), determined from nitrogen adsorption isotherms at 77 K (Table II), confirmed the material morphology change as a function of the synthesis method. According to these results, a ~7-fold increase of both parameters was observed for the KNb_3O_8 synthesized by the PP method in relation to the SS one. The BET surface area for the material synthesized by SS method was compatible with the literature [14, 20, 21].

CONCLUSIONS

The polymer precursor method was successfully used

Table II - BET surface area (S_{BET}) and total pore volume (V_p), determined from nitrogen adsorption isotherms at 77 K, of KNb_3O_8 synthesized by PP method heat treated at 750 °C and by the SS method.
[Tabela II - Área superficial de BET (S_{BET}) e volume total de poros (V_p), determinados por isotermas de adsorção de nitrogênio a 77 K, do KNb_3O_8 sintetizado pelo método PP, tratado a termicamente 750 °C, e pelo método SS.]

Synthesis method	S_{BET} ($m^2.g^{-1}$)	V_p ($cm^3.g^{-1}$)
SS	1.4	$1.9x10^{-3}$
PP	9.5	$14x10^{-3}$

for the synthesis of KNb_3O_8 with important advantages in relation to the solid-state method, as the absence of secondary phases besides higher surface area and higher pore volume, which may be useful for catalytic processes. Moreover, the polymeric precursor method requires lower heat treatment temperatures and heating periods.

ACKNOWLEDGEMENTS

Authors acknowledge the Brazilian funding agencies CAPES and CT-INFRA/FINEP/MCTIC for the financial support of this work, CBMM by the cession of the niobium precursors, Laboratório de Tecnologia de Novos Materiais, IDEP-UFPB (SEM analysis) and F. Gouttefangeas and L. Joanny for SEM images performed at CMEBA (ScanMAT, University of Rennes 1).

REFERENCES

[1] Z.Y. Zhan, C.Y. Xu, L. Zhen, W.S. Wang, W.Z. Shao, Ceram. Int. **36** (2010) 679.
[2] L. Li, J. Deng, R. Yu, J. Chen, X. Wang, X. Xing, Inorg. Chem. **49**, 4 (2010) 1397.
[3] K. Kakimoto, K. Sugiyama, I. Kagomiya, J. Ceram. Soc. Jpn. **118**, 8 (2010) 696.
[4] G. Zhang, J. Gong, H. Gan, F. Lü, J. Alloys Compd. **509** (2011) 9791.
[5] S. Suzuki, K. Teshima, A. Yamaguchi, K. Yubuta, T. Shishido, S. Oishi, Cryst. Eng. Comm. **14** (2012) 987.
[6] G. Zhang, J. Gong, X. Zou, F. He, H. Zhang, Q. Zhang, Y. Liu, X. Yang, B Hu, Chem. Eng. J. **123** (2006) 59-64.
[7] G. Zhang, F. He, X. Zou, J. Gong, H. Tu, H. Zhang, Q. Zhang, Y. Liu, J. Alloys Compd. **427** (2007) 82.
[8] M. Gasperin, Acta. Cryst. **B38** (1982) 2024.
[9] K. Momma, F. Izumi, J. Appl. Crystallogr. **44** (2011) 1272.
[10] M.A. Bizeto, D.L.A. de Faria, V.R.L. Constantino, J. Mater. Sci. Lett. **18** (1999) 643.
[11] L. Li, J. Deng, J. Chen, X. Sun, R. Yu, G. Liu, X. Xing, Chem. Mater. **21** (2009) 1207.
[12] J. Liu, X. Li, Y. Li, J. Cryst. Growth **247** (2003) 419.
[13] T.M. Duarte, L.M.C. Honorio, A.S. Brito, J.K.D. Souza, E. Longo, R.L. Tranquilin, A.G. Souza, I.M.G. Santos, A.S. Maia, Mater. Sci. Eng. R **97** (2015) 012001.
[14] X. Li, H. Pan, W. Li, Z. Zhuang, Appl. Catal. A: General, **413-414** (2012) 103.
[15] L. Zhang, Y. Hou, M. Zheng, M. Zhu, H. Yan, Mater. Chem. Phys. **149-150** (2015) 418.
[16] G. Yang, Y. Kong, W. Hou, Q. Yan, J. Phys. Chem. B **109** (2005) 1371.
[17] A. Kudo, T. Sakata, J. Phys. Chem. **100** (1996) 17323.
[18] B. Yu, B. Cao, H. Cao, X. Zhang, D. Chen, J. Qu, H. Niu, Nanotechnology **24** (2013) 085704.
[19] J. Jehng, I.E. Wachs, Chem. Mater. **3** (1991) 100.
[20] A. Takagaki, D. Lu, J.N. Kondo, M. Hara, S. Hayshi, K. Domen, Chem. Mater. **17** (2005) 2487.
[21] S. Liang, L. Wen, S. Lin, J. Bi, P. Feng, X. Fu, L. Wu, Angew. Chem. Int. Ed. **53** (2014) 2951.
(Rec. 31/03/2017, Rev. 03/05/2017, 16/06/2017, Ac. 06/07/2017